In-Vivo Time-Resolved Autofluorescence Measurements on Human Skin

Kamal M. Katika[a], Laurent Pilon[a], Katrina Dipple[b], Seymour Levin[c], Jennifer Blackwell[a] and Halil Berberoglu[a]

[a]Mechanical and Aerospace Engineering Department, Henri Samueli School of Engineering and Applied Science, University of California, Los Angeles, Los Angeles, CA 90095;
[b]Departments of Human Genetics and Pediatrics, David Geffen School of Medicine, University of California, Los Angeles, Los Angeles, CA 90095;
[c] Wadsworth Veterans Administration Hospital, Los Angeles, CA 90073;

ABSTRACT

In this paper we present preliminary results obtained from fluorescence lifetime measurements on human skin using time-correlated single photon counting (TCSPC) techniques. Human skin was exposed to light from a pulsed LED of 700 ps pulse width at a wavelength of 375 nm and fluorescence decays were recorded at four different emission wavelengths (442, 460, 478 and 496 nm) using a photomultiplier tube (PMT) coupled to a monochromator. Measurements were carried out on the left and right palms of subjects recruited for the study after obtaining consent using a UCLA IRB approved consent form. The subjects recruited consisted of 18 males and 17 females with different skin complexions and ages ranging from 10 to 70 years. In addition, a set of experiments were also performed on various locations including the palm, the arm and the cheek of a Caucasian subject. The fluorescence decays thus obtained were fit to a three-exponential decay model in all cases and were approximately 0.4, 2.7 and 9.4 ns, respectively. The variations in these lifetimes with location, gender, skin complexion and age are studied. It is speculated that the shorter lifetimes correspond to free and bound NADH while the longer lifetime is due to AGE crosslinks.

Keywords: fluorescence, autofluorescence, time-resolved fluorescence, skin

1. INTRODUCTION

Fluorescence is the physical phenomenon in which light is emitted by a substance as a result of excited electrons returning to their ground states after absorption of excitation light. Biological tissues contain several endogenous fluorophores such as NADH, aromatic amino acids like tryptophan and structural proteins such as collagen and elastin [1]. The optical properties of these fluorophores are sensitive to the environment and the metabolic status of the tissue thus, making fluorescence spectroscopy a valuable tool to study the health of biological tissues. Fluorescence spectroscopy consists of measuring the fluorescent intensity emitted by fluorophores after being excited by light at a suitable wavelength and can be performed in a steady-state or time-resolved manner. Steady-state measurements typically involve either measuring the emission or excitation spectra. Fluorescence emission spectrum measurements consist of measuring the fluorescence intensity over a range of wavelengths for a fixed excitation wavelength. On the contrary, excitation spectra measurements consist of measuring the fluorescence intensity at a particular wavelength for a range of excitation wavelengths.

Time-resolved measurements involve measuring the lifetime of the fluorophores and are much more complex than steady-state spectral measurements due to the instrumentation required. Even though steady-state measurements are relatively easy to perform, they present some limitations, (i) they measure the fluorescence intensity integrated over time and therefore, lose the information associated with the dynamics of the fluorescence process and (ii) they are intensity dependent and therefore are sensitive to excitation light intensity, to optical

Further author information:(Send correspondence to Laurent Pilon.)
Kamal M. Katika: E-mail: kamal@seas.ucla.edu
Laurent Pilon: E-mail: pilon@seas.ucla.edu

losses in the experimental setup, and to absorption and scattering by tissue [2] . Time-resolved measurements, on the other hand, capture the transient decay which depends on the relative concentrations and lifetimes of the fluorophores contributing to the fluorescence signal [2]. Also, they are extremely sensitive to the local biochemical environment such as the *p*H and oxygenation which may differ in healthy and diseased tissue [2]. In addition, the fluorophore lifetimes are independent of absolute intensity and so do not change with variations in excitation intensity or optical losses from hemoglobin absorption [2]. Finally, fluorescence lifetime measurements enable the discrimination of fluorophores with overlapping emission spectra but different lifetimes [3]. For example, various tryptophan residues in proteins have similar emission spectra but different lifetimes and thus can be distinguished by time-resolved fluorescence measurements [4].

Time-resolved fluorescence techniques can be performed either in frequency-domain or in time-domain [4], each with their own advantages and disadvantages depending on the experimental setting. Frequency-domain techniques involve exciting the sample with a sinusoidally modulated source which could be a continuous wave laser or a flash lamp, and measuring the phase shift of the emitted light at multiple excitation frequencies to compute the fluorescence lifetime [4]. Alternatively, time-domain measurements typically use ultra-short pulsed light to excite the sample and measure the emitted fluorescence as a function of time, thus enabling one to compute the lifetime of the fluorophore. Note that, the pulse width must be of the same order of magnitude or shorter than the fluorescence lifetime. Time-domain measurements are preferred in a clinical setting for the following reasons, (i) they feature short acquisition times compared to frequency-domain measurements [3] and (ii) they are insensitive to ambient light at the collection site [3].

The goal of the present study is to measure fluorescence lifetimes on human skin *in-vivo* using time-domain techniques for their advantages, and study the effect of various parameters such as sensing location, complexion and gender on the recovered lifetimes. This work would be of particular importance to studies on skin autofluorescence measurements for non-invasive glucose sensing [5] and the design of implantable glucose sensors based on fluorescence. It would also serve as a baseline for using time-resolved autofluorescence of human skin to monitor diseases and conditions such as diabetes, skin cancer, wounds, and ulcers.

2. CURRENT STATE OF KNOWLEDGE

This section reviews experimental studies of time-resolved fluorescence measurements of biological tissues. *In-vivo* time-resolved fluorescence measurements have come into prominence only recently and a limited number of studies have been reported in the literature and summarized in Table 1. For example, Pradhan *et al.* [6] have used fluorescence lifetime measurements to study breast tissue. They made use of laser pulses of 100 fs pulse width at 310 nm and a streak camera to obtain a 2D map of the fluorescence lifetimes. It was shown that time-resolved fluorescence measurements at an emission wavelength around 340 nm can be used to distinguish malignant tumors from non-malignant breast tissues.

Fluorescence lifetime measurements have also been used to study tissue during endoscopy. Glanzmann *et al.* [7] described a time-resolved fluorescence instrument based on pumped laser excitation sources and a streak camera coupled to a spectrograph as a detector. The instrument was used to measure the fluorescence decays of endogenous fluorophores and of ALA (δ-aminolevulinic acid) induced protoporphyrin IX (PPIX) in an excised human bladder with a carcinoma. The authors were able to correctly identify healthy tissue which appeared as abnormal in steady-state spectroscopy. The instrument was then used to perform in-situ characterization during endoscopy and time-resolved spectra of tissue fluorescence of the human bladder, the bronchi, and the esophagus were obtained [8]. Further studies were conducted by the same group [9] to test the viability of fluorescence lifetime as a new contrast parameter between normal and malignant tissue in the bronchi. However, they were unable to obtain a contrast in the fluorescence lifetime or the spectrum between normal and moderately dysplasic tissue in the spectral region between 510 and 650 nm. Mizeret *et al.* [10] also studied the feasibility of performing endoscopic fluorescence lifetime measurements using frequency modulation techniques in real time in a clinical setting. The instrument made use of an excitation source at 514.5 nm and a detection unit consisting of CCD units with image intensifier tubes. Fluorescence lifetime values for healthy bronchial tissue were reported. Moreover, Pfefer *et al.* [11] performed *in-vivo* fluorescence lifetime and spectral measurements on patients undergoing routine endoscopic surveillance for Barrett's esophagus. A time-domain instrument consisting of a laser pulsing at 337 nm and a pulse width of 3 ns and an avalanche photodiode coupled to an oscilloscope was used in the experiments.

The excitation wavelengths used were 337 nm and 400 nm and the emission was collected around 550 nm. It was found that low risk tissue and high grade dysplasia could not be differentiated based on time-resolved fluorescence data.

Furthermore, Schweitzer and co-workers [12, 13] performed fluorescence lifetime studies on the human ocular fundus. They made use of time correlated single photon counting (TCSPC) techniques with a pulsed laser of 300 ps pulse width at a wavelength of 457.9 nm and various emission wavelength ranges. They obtained a lifetime of 1.5 ns in the para-papillary region of the eye and a lifetime of 5 ns in the optical disc which they attributed to collagen. They also showed that breathing 100% oxygen affects the fluorescence lifetimes and speculated that the lifetime of fluorophores present in the retinal pigment epithelium depends on the oxygen supply.

Fluorescence lifetime measurements have also been performed on tissue *in-vitro*. For example, Maarek *et al.* [14] used time-domain *in-vitro* fluorescence lifetime measurements and spectroscopy for diagnosis of atherosclerotic lesions. The instrument consisted of an excitation laser at 337 nm and a pulse width of 3 ns, a microchannel plate photomultiplier attached to a monochromator and connected to a digital oscilloscope. Fluorescence lifetimes were measured at emission wavelengths ranging from 370 nm to 510 nm. They were able to discriminate between stable and unstable lesions by studying the time-resolved spectra of components present in the arterial wall, namely, structural proteins like collagen, lipoproteins and cholesterol [15].

Moreover, Cubeddu and co-workers [16, 17] used fluorescence lifetime imaging (FLIM) to study tumors in human skin. The instrumentation consisted of a dye laser pulsing at 405 nm at a pulse width of less than 1 ns and a gated imaging system. An exogeneous marker was used to induce selective accumulation of PPIX in proliferative tissue. Thus tumors were identified using lifetime imaging thanks to the longer fluorescence lifetime of PPIX (18 ns) compared to that of healthy tissue ($\sim$ 10 ns). Siegel *et al.* [18] also used FLIM techniques using a pulsed laser at 415 nm and a pulse width less than 100 fs and a gated optical intensifier to image the autofluorescence from various biological tissue *in-vitro* including animal tissue, knee joints, and human teeth. Using this instrument they were able to distinguish the tendon, bone, and surrounding tissue which was not possible using white light and steady-state fluorescence measurements. Similarly, they showed that various regions in an extracted human tooth can be clearly distinguished using FLIM unlike reflectance and steady-state fluorescence measurements.

Finally, studies have measured the time-resolved fluorescence of human skin. Konig and co-workers [19–21] used 3D autofluorescence lifetime imaging and investigated various tissues of patients with psoriasis, nevi, dermatitis, basalioma, and melanoma *in vitro* as well as the skin of healthy subjects *in-vivo*. Their system was able to achieve a sub-cellular spatial resolution and a temporal resolution of 250 ps. The authors analyzed the fluorescence decays from images obtained at various depths of the skin and reported lifetimes of around 1.85 ns at the stratum corneum and a lifetime of about 2.4 ns at a depth of 50 μm within the stratum spinosum. In addition, Pitts and Mycek [2] described a time-domain instrument with both spectral and temporal resolution to measure fluorescence lifetimes and emission spectrum *in-vivo* and *in-vitro*. The instrument was based on a pumped dye laser with a pulse width of 4 ns as an excitation source and an avalanche photo diode along with a 1 GHz oscilloscope as a detector. Fluorescence lifetime measurements were performed on human skin *in-vivo* at an excitation wavelength of 337 nm and an emission wavelength of 460 nm. The time-resolved data was fit to a double-exponential decay yielding lifetimes of 0.938 ns and 5.3 ns. The longer lifetime was attributed to the emission from collagen. The instrument was also used to measure fluorescence lifetimes of biomolecules present in human cells.

In this paper we present the construction of a device to measure fluorescence lifetimes on human skin *in-vivo* using the principle of Time Correlated Single Photon Counting (TCSPC). The device was tested on 35 healthy subjects of different age, gender, and skin complexion after obtaining UCLA IRB approved consent. The fluorescence lifetimes were measured on the palms of subjects at an excitation wavelength of 375 nm and at four emission wavelengths. Moreover, experiments were also performed on the palms, the arms, the feet,and the cheeks of a 31 year old Caucasian subject. Finally, the possible origin of these fluorescence lifetimes is discussed. To the best of our knowledge, this is the first comprehensive study reporting fluorescence lifetimes of human skin measured *in-vivo* on subjects of different ages, gender, and skin complexions.

3. EXPERIMENTAL APPARATUS

The present study made use of the TCSPC technique to measure fluorescence lifetimes of skin. A sensing head was constructed to simultaneously excite the sample and collect the resulting fluorescence emission. The sensing head was designed such that excitation light was incident normally on the sample while fluorescence emission was collected at an angle of 45° from the normal. The sample surface was shielded from ambient light. Excitation and emission light were channeled by means of liquid light guides attached to the sensing head. Liquid light guides were used to transmit the excitation and fluorescence light instead of commonly used fiber optics as the transmission and coupling efficiency of these are higher compared to fiber optics.

A schematic of the experimental setup is shown in Figure 1. The excitation source used in the experiments was a light emitting diode or LED (PLS 370 diode, PicoQuant GmbH) with its center wavelength at 375 nm with a spectral width of around 10 nm. The full width half maximum of the diode pulses at a repetition rate of 2.5 MHz and average power of 4.8 μW was 664 ps. The LED was driven by a diode driver (PDL-800 B diode driver, PicoQuant GmbH) at a repetition rate of 5 MHz. A liquid light guide designed for the UV-visible part of the spectrum (77628, from Spectra-Physics, U.S.A) carried light from the LED to the sensing head while another liquid light guide designed for the visible part of the spectrum (77631, from Spectra-Physics, U.S.A), was used to collect the fluorescence emission and carry it to a monochromator (SpectraPro-150, Acton Research Corporation, U.S.A.). A photomultplier tube (PMT) assembly (PMA-M 165 from PicoQuant GmbH) was coupled to the monochromator on the other end. The monochromator slits on the entry and exit of the light path were adjusted manually to maintain a bandwidth of 3 nm. For the data acquisition, the "sync" output

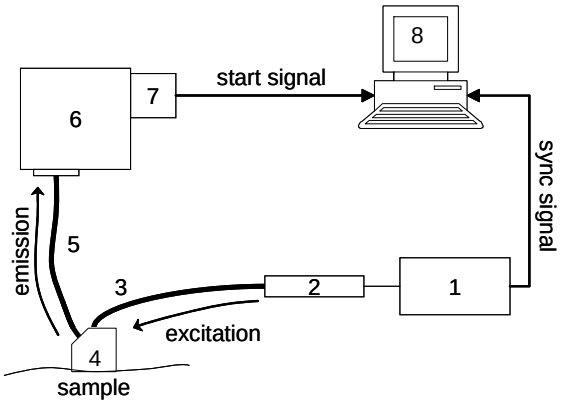

Figure 1. A schematic of the experimental set-up, (1) diode driver, (2) LED, (3) liquid light guide, (4) sample probe, (5) liquid light guide, (6) monochromator, (7) photomultiplier tube, and (8) personal computer

signal from the diode driver and the "start" signal from the PMT assembly were fed to the respective channels on the data acquisition board (TimeHarp 200 from PicoQuant GmbH), via standard 50 Ohms coaxial cables. The "sync" output from the diode driver provided the signal to synchronize the timing electronics on the data acquisition board mounted on a personal computer (PC).

4. TESTING PROCEDURE AND OPTIMIZATION OF MEASUREMENT PARAMETERS

The measurement procedure and parameters were arrived at by conducting preliminary studies on the palms, the arms, the cheeks and feet of a 31 year old male Caucasian subject as well as from other studies reported in literature. The fluorescence lifetimes were measured at four different emission wavelengths, namely 442 nm, 460 nm, 478 nm and 496 nm. The first wavelength was chosen based on studies reported in literature. It was found that collagen fluorescence exhibited a maximum at around 440 nm when excited by light at 370 nm corresponding to collagenase-digestible collagen cross-links [22]. The remaining wavelengths were arbitrarily chosen to cover the spectral range up to 500 nm.

In order to measure the fluorescence lifetimes, the monochromator was set to the emission wavelength of interest and the monochromator slits were adjusted to match that particular wavelength. The probe was then placed on the skin surface and the LED was turned on. The PMT shutter was opened once the sensing head was firmly placed on the skin surface and then the histograms were collected using the TimeHarp software. The probe was held in contact with the palm till 1500 counts were acquired in the peak channel. This number was arrived at by considering a trade-off between the duration of the experiments and the signal to noise ratio. The duration of a single measurement ranged from 5 minutes to 20 minutes based on the sensing location and emission wavelength. It was observed that the time taken for each measurement was least on the palm, possibly due to the low concentration of melanin. Moreover, higher emission wavelengths required longer durations to achieve these counts due to a lower intensity of the fluorescence. The instrument response function (IRF) was measured by placing the probe on a teflon block for the same number of maximum counts as in the *in-vivo* measurements. The deconvolution software FluoFit version 4.0 was used to recover the lifetimes from the measured fluorescence decays that were then curve fit to a multi-exponential model. An attempt was made to fit the decays to a single-exponential, a bi-exponential model and a tri-exponential model. Only the bi-exponential model and the tri-exponential model gave a value of χ^2 around 1.0 which indicated a good fit. However, the bi-exponential model was rejected in favor of the more complicated tri-exponential model due to the presence of oscillations in the plot of the residuals compared to more random residuals for the tri-exponential model. Thus, the fluorescence decay could be modeled as

$$F(t) = A_1 e^{-t/\tau_1} + A_2 e^{-t/\tau_2} + A_3 e^{-t/\tau_3} \quad (1)$$

Table 2 presents a statistical summary of the six fluorescence lifetime measurements on the left palm of this subject at an emission wavelength of 442 nm. These experiments were performed over a period of 1 month and different times of the day. The coefficient of variation which represents the variation in measurements is less than 5% in all cases except for the parameters τ_1 and A_3 for which it reaches 7% and 15%, respectively.

Finally, measurements were also taken on the inner arms, the cheeks and the feet of the same subject. Figure 2 shows the fluorescence lifetimes τ_1, τ_2, and τ_3 and their corresponding amplitudes A_1, A_2, and A_3 obtained as a function of wavelength and sensing location, namely, the palms, the arms, the cheeks and the feet. The plots seem to indicate that the fluorescence lifetimes do not vary significantly with location and wavelength. Further tests are needed to assess whether the differences are statistically insignificant. In the remainder of the document, only the results for an emission wavelength of 442 nm are presented. Similar trends are observed for other emission wavelengths.

5. PRELIMINARY DATA

The instrument was then tested on 35 human subjects after obtaining UCLA IRB approved consent. The subjects consisted of 18 males and 17 females ranging from 10 to 70 years of age. Of these, there were 17 Caucasians, 4 African-Americans, 6 Asians, and 8 Hispanics. The palms were chosen as the sensing location for these subjects due to the shorter duration of the experiments as well as being accessible. The first measurement at 442 nm was performed on the left palm and subsequent measurements at higher wavelengths were performed alternately on the right and left palms. Figure 3 shows the raw data of the fluorescence lifetimes and their corresponding amplitudes for 35 subjects of various ages, genders, and skin complexion at an emission wavelength of 442 nm. The error bars represent asymptotic standard errors in the fluorescence lifetimes obtained using the Fluofit software package. A preliminary statistical analysis was performed on the data to determine the average values of the fluorescence lifetimes and the amplitudes which might serve as a baseline. Table 3 presents the mean values and the standard deviations of the fluorescence lifetimes and their corresponding amplitudes. In order to further analyze the fluorescence lifetime data obtained, various factors varying from one individual to another, namely, (i) skin complexion (ii) gender, and (iii) age were considered.

5.1. Effect of Skin Complexion and Gender

Figure 4 shows the fluorescence lifetimes τ_1, τ_2, and τ_3 as a function of age and skin complexion for subjects in the age group of 30 to 40 years at an emission wavelength of 442 nm. It indicates that the fluorescence lifetimes do not significantly vary for different skin complexions. Moreover Figure 5 shows the fluorescence lifetimes as a function of age and gender for subjects in the same age group at the same emission wavelength. Again there are

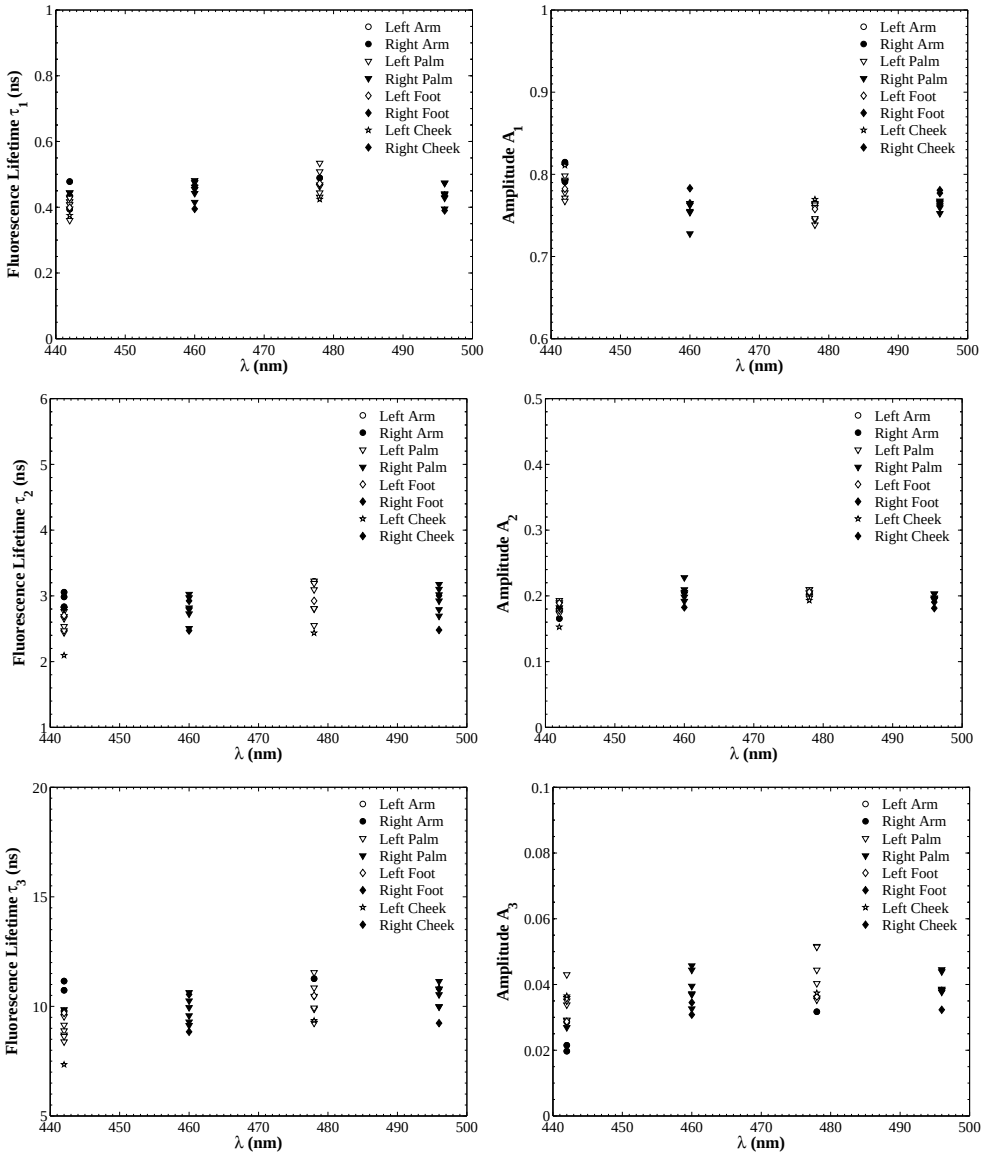

Figure 2. Effect of sensing location on fluorescence lifetimes τ_1, τ_2 and τ_3 and amplitudes A_1, A_2 and A_3 as a function of wavelength for a male 31 year old Causcasian subject.

no noticeable trends in the fluorescence lifetimes with respect to gender. Thus, this preliminary data indicates that fluorescence lifetimes do not vary with skin complexion and gender. Similar trends were observed at other emission wavelengths.

5.2. Effect of Age

Finally, an attempt was made to model the fluorescence lifetimes shown in Figure 3 as a function of age using linear regression. The square of the correlation coefficient, R^2 was less than 0.03 for all three lifetimes, thus indicating that variations in fluorescence lifetimes with age cannot be described by a linear model. Moreover, the small regression coefficients in all the cases also indicate that the three lifetimes do not depend on the age of the individual. While the presented regression analysis is a simplistic model, it lays the foundation to more

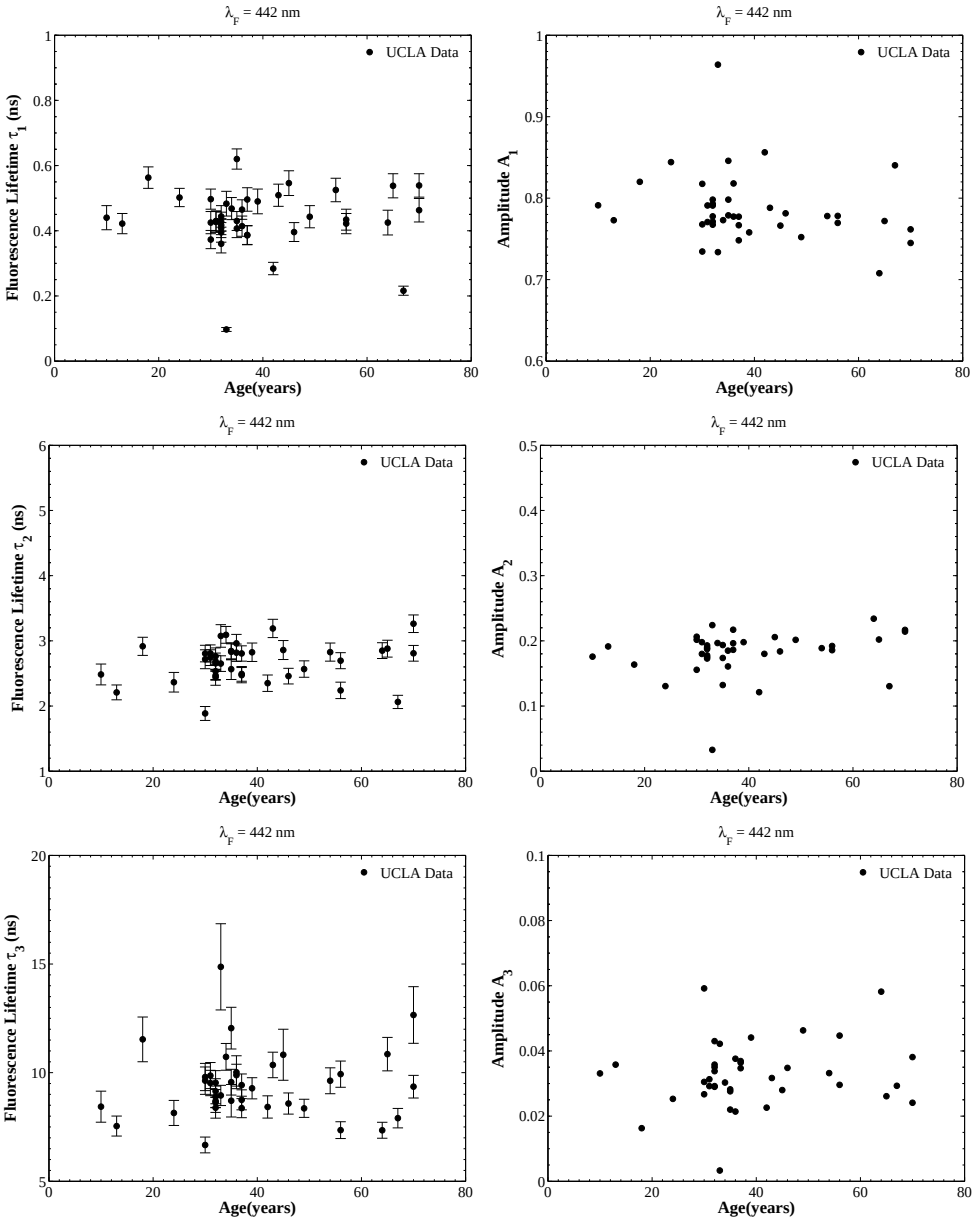

Figure 3. Effect of age on the fluorescence lifetimes τ_1, τ_2 and τ_3 and amplitudes A_1, A_2 and A_3 for healthy subjects at an emission wavelength of 442 nm.

sophisticated models capturing various other factors which can alter the autofluorescence of human skin such as diabetes and skin cancer .

5.3. Identification of Fluorophores

In an earlier study on fluorescence lifetime measurements on human skin [2], two fluorescence lifetimes of 0.938 ns and 5.3 ns were reported and the longest lifetime was attributed to collagen [2]. In the present study, similar values were found when the decays were fit to a bi-exponential model. However, as mentioned earlier, this model was rejected in favor of a tri-exponential model. Moreover, the shorter two lifetimes τ_1 around 0.4 ns and τ_2 around 2.7 ns observed in our measurements were close to the lifetimes of free and bound NADH reported in

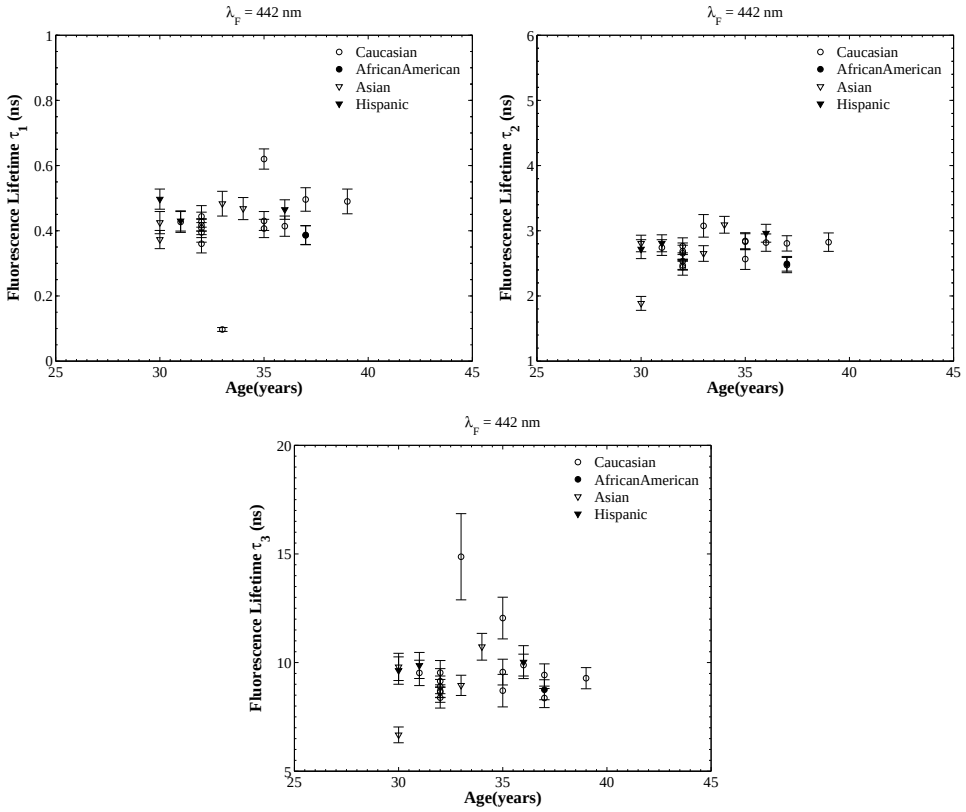

Figure 4. Effect of skin complexion on the fluorescence lifetimes τ_1, τ_2 and τ_3 as a function of age for healthy subjects at an emission wavelength of 442 nm.

literature [20,23]. Indeed, Schneckenburger [23] studied the autofluorescence from cultivated endothelial cells and determined the fluorescence lifetime of free and protein bound NADH to be 0.4-0.5 ns and 2.0-2.5 ns respectively. Furthermore Konig and Riemann [20] also reported a fluorescence lifetime of 2.7 ns at a depth of 50 μm within the skin which could possibly be due to bound NADH. Based on these studies, it is speculated that the two shorter fluorescence lifetimes τ_1 and τ_2 correspond to free and bound NADH. Furthermore, it is speculated that the third observed lifetime $\tau_3 = 9.4$ ns corresponds to collagen crosslinks formed by advanced glycation endproducts (AGEs) [24,25]. Further *in-vitro* experiments are needed to verify these speculations.

6. CONCLUSIONS

This paper presented the experimental apparatus assembled to measure autofluorescence lifetimes of human skin. The assembled device was tested on 35 subjects recruited at UCLA. Skin autofluorescence lifetimes were obtained from these subjects and the effect of several factors such as age, sensing location, and skin complexion were explored. In all cases, the fluorescence decay was fit to a multi-exponential model with three fluorescence lifetimes of 0.4 ns, 2.7 ns, and 9.4 ns. A preliminary statistical analysis on the fluorescence lifetimes obtained on the inner arm and the palm of a 31 year old male Caucasian subject indicated differences in τ_2 and τ_3 while there were no differences in τ_1. However, they were independent of the skin complexion and the gender of the subjects. Moreover, it is speculated that the shorter two fluorescence lifetimes correspond to free and bound NADH while the longer lifetime corresponds to AGE crosslinks. This study is of particular interest especially with the possibility of using fluorescence lifetimes of NADH to non-invasively sense glucose concentrations [5] as well as monitoring diseases and skin conditions such as diabetes, skin cancer, wounds, and ulcers.

[h]

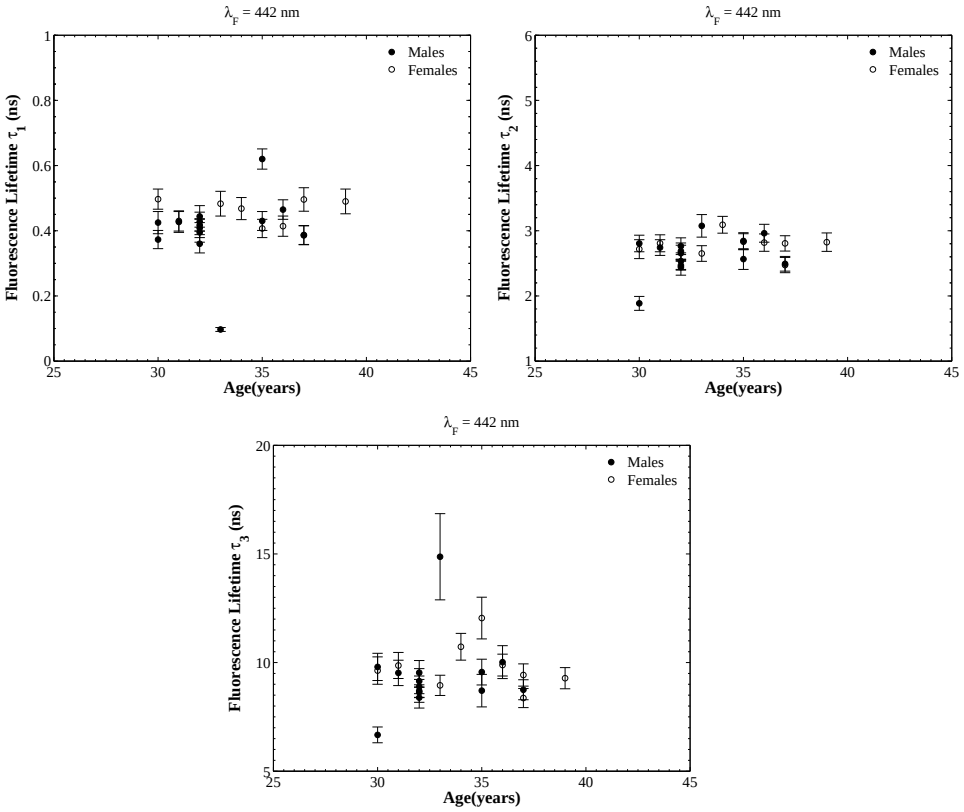

Figure 5. Effect of gender on the fluorescence lifetimes τ_1, τ_2 and τ_3 as a function of age for healthy subjects at an emission wavelength of 442 nm.

7. ACKNOWLEDGEMENTS

The authors would like to thank Bill Van Antwerp of Medtronic Minimed for his invaluable inputs to this present study.

REFERENCES

1. R. Richards-Kortum and E. Sevick-Muraca, "Quantitative optical spectroscopy for tissue diagnostics," *Annual Review of Physical Chemistry* **47**, pp. 555–606, 1996.
2. J. D. Pitts and M.-A. Mycek, "Design and development of a rapid acquisition laser-based fluorometer with simultaneous spectral and temporal resolution," *Review of Scientific Instruments* **72**, pp. 3061–3072, 2001.
3. Q. Fang, T. Papaioannou, J. A. Jo, R. Vaitha, K. Shastry, and L. Marcu, "Time-domain laser-induced fluorescence spectroscopy apparatus for clinical diagnostics," *Review of Scientific Instruments* **75**(1), pp. 151–162, 2004.
4. J. R. Lakowicz, *Principles of Fluorescence Spectroscopy*, Kluwer Academic/Plenum Publishers, New York, NY, 1999.
5. N. Evans, L. Gnudi, O. Rolinski, D. Birch, and J. Pickup, "Glucose-dependent changes in NAD(P)H-related fluorescence lifetime of adipocytes and fibroblasts in vitro: Potential for non-invasive glucose sensing in diabetes mellitus," *Journal of Photochemistry and Photobiology B: Biology* **80**(2), pp. 122–129, 2005.
6. A. Pradhan, B. B. Das, K. M. Yoo, R. R. Alfano, J. Cleary, R. Prudente, and E. J. Celmer, "Time-resolved fluorescence of benign and malignant breast tissues," *Proceedings of the SPIE* **1599**(1), pp. 81–84, 1992.

7. T. M. Glanzmann, J.-P. Ballini, P. Jichlinski, H. van den Bergh, and G. A. Wagnieres, "Tissue characterization by time-resolved fluorescence spectroscopy of endogenous and exogenous fluorochromes: apparatus design and preliminary results," *Proceedings of the SPIE* **2926**, pp. 41–50, 1996.
8. T. Glanzmann, J.-P. Ballini, H. van den Bergh, and G. Wagnieres, "Time-resolved spectrofluorometer for clinical tissue characterization during endoscopy," *Review of Scientific Instruments* **70**, pp. 4067–4077, 1999.
9. T. M. Glanzmann, P. Uehlinger, J.-P. Ballini, A. Radu, T. Gabrecht, P. Monnier, H. van den Bergh, and G. A. Wagnieres, "Time-resolved autofluorescence spectroscopy of the bronchial mucosa for the detection of early cancer: clinical results," *Proceedings of the SPIE* **4432**, pp. 199–209, 2001.
10. J. Mizeret, T. Stepinac, M. Hansroul, A. Studzinski, H. van den Bergh, and G. Wagnieres, "Instrumentation for real-time fluorescence lifetime imaging in endoscopy," *Review of Scientific Instruments* **70**, pp. 4689–4701, 1999.
11. T. J. Pfefer, D. Y. Paithankar, J. M. Poneros, K. T. Schomacker, and N. S. Nishioka, "Temporally and spectrally resolved fluorescence spectroscopy for the detection of high grade dysplasia in Barrett's esophagus," *Lasers in Surgery and Medicine* **32**(1), pp. 10–16, 2003.
12. D. Schweitzer, A. Kolb, M. Hammer, and E. Thamm, "Tau-mapping of the autofluorescence of the human ocular fundus," *Proceedings of the SPIE* **4164**, pp. 79–89, 2000.
13. D. Schweitzer, A. Kolb, and M. Hammer, "Autofluorescence lifetime measurements in images of the human ocular fundus," *Proceedings of the SPIE* **4432**, pp. 29–39, 2001.
14. J.-M. I. Maarek, L. Marcu, M. C. Fishbein, and W. S. Grundfest, "Time-resolved fluorescence of human aortic wall: Use for improved identification of atherosclerotic lesions," *Lasers in Surgery and Medicine* **27**, pp. 241–254, 2000.
15. L. Marcu, W. S. Grundfest, and J.-M. I. Maarek, "Arterial fluorescent components involved in atherosclerotic plaque instability: differentiation by time-resolved fluorescence spectroscopy," *Proceedings of the SPIE* **4244**, pp. 428–433, 2001.
16. R. Cubeddu, A. Pifferi, P. Taroni, A. Torricelli, G. Valentini, and E. Sorbellini, "Fluorescence lifetime imaging: an application to the detection of skin tumors," *IEEE Journal of Selected Topics in Quantum Electronics* **5**(4), pp. 122–132, 1999.
17. R. Cubeddu, D. Comelli, C. D'Andrea, P. Taroni, and G. Valentini, "Clinical system for skin tumour detection by fluorescence lifetime imaging," *Engineering in Medicine and Biology* **3**, pp. 2295 – 2296, 2002.
18. J. Siegel, D. S. Elson, S. E. D. Webb, K. C. B. Lee, A. Vlandas, G. L. Gambaruto, S. L.-Fort, M. J. Lever, P. J. Tadrous, G. W. H. Stamp, A. L. Wallace, A. Sandison, T. F. Watson, F. Alvarez, and P. M. W. French, "Studying biological tissue with fluorescence lifetime imaging: microscopy, endoscopy, and complex decay profiles," *Applied Optics* **42**(16), pp. 2995–3004, 2003.
19. K. Koenig, U. Wollina, I. Riemann, C. Peukert, K.-J. Halbhuber, H. Konrad, P. Fischer, V. Fuenfstueck, T. W. Fischer, and P. Elsner, "Optical tomography of human skin with subcellular spatial and picosecond time resolution using intense near infrared femtosecond laser pulses," *Proceedings of the SPIE* **4620**, pp. 191–201, 2002.
20. K. Konig and I. Riemann, "High-resolution multiphoton tomography of human skin with subcellular spatial resolution and picosecond time resolution," *Journal of Biomedical Optics* **8**(3), pp. 432–439, 2003.
21. I. Riemann, E. Dimitrov, P. Fischer, A. Reif, M. Kaatz, P. Elsner, and K. Konig, "High-resolution multiphoton tomography of human skin in vivo and in vitro," *Proceedings of the SPIE* **5463**, pp. 21–28, 2004.
22. R. H. Na, I. M. Stender, M. Henriksen, and H. C. Wulf, "Autofluorescence of human skin is age-related after correction for skin pigmentation and redness," *Journal of Investigative Dermatology* **116**, pp. 536–540, 2001.
23. H. Schneckenburger, M. Wagner, P. Weber, W. S. Strauss, and R. Sailer, "Autofluorescence Lifetime Imaging of Cultivated Cells Using a UV Picosecond Laser Diode," *Journal of Fluorescence* **14**(5), pp. 649 – 654, 2004.
24. R. Meerwaldt, R. Graaff, P. H. N. Oomen, T. P. Links, J. J. Jager, N. L. Alderson, S. R. Thorpe, J. W. Baynes, R. O. B. Gans, and A. J. Smit, "Simple non-invasive assessment of advanced glycation endproduct accumulation," *Diabetologia* **47**, pp. 1324–1330, 2004.

25. E. Hull, M. Ediger, A. Unione, E. Deemer, M. Stroman, and J. Baynes, "Noninvasive, optical detection of diabetes: model studies with porcine skin," *Optics Express* **12**(19), pp. 4496–4510, 2004.
26. D. Schweitzer, M. Hammer, F. Schweitzer, R. Anders, T. Doebbecke, S. Schenke, E. R. Gaillard, and E. R. Gaillard, "In vivo measurement of time-resolved autofluorescence at the human fundus," *Journal of Biomedical Optics* **9**(6), pp. 1214–1222, 2004.

Table 1. Experimental studies of time-resolved fluorescence spectroscopy on human tissues.

Ref	**Excitation Wavelength**	**Emission Wavelength**	**Spectroscopy method**	**Sensing region**	***in-vivo*/ *in-vitro***
[**2**]	337.1 nm	N.A	time-domain using an APD and fast oscilloscope	human skin	*in-vivo*
[**6**]	310 nm	340 and 440 nm	time-domain using a streak camera	breast tissue	*in-vitro*
[**7**]	337.1 nm 425, 476 and 500 nm	500-680nm	time-domain using a streak camera	human bladder	*in-vitro*
[**8**]	337.1 nm, 480 nm	375-515 nm, 525-615 nm	time-domain using a streak camera	bladder, bronchii, oesophagus	*in-vivo*
[**9**]	406 nm	430-680 nm	time-domain using a streak camera	bronchii	*in-vivo*, endoscopy
[**10**]	514.5 nm	550-650 nm	frequency domain	bronchii	*in-vivo*, endoscopy
[**11**]	337 nm, 400 nm	550 nm	time-domain using a gated intensified diode array	esophagus	*in-vivo*, endoscopy
[**12, 13, 26**]	458 nm, 446 nm	510-700 nm	time-domain using TCSPC	human ocular fundus	*in-vivo*
[**14, 15**]	337.1nm	370-510 nm	time-domain using a transient digitizer	aorta, and its components	*in-vitro*
[**16, 17**]	405 nm	N.A	time-domain using time gating	skin tumors	*in-vitro*
[**18**]	415 nm	N.A	time-domain using time gating	rabbit knee joint and human tooth	*in-vitro*
[**19–21**]	750-850 nm	N.A	time-domain using TCSPC	human skin	*in-vivo*

Table 2. Statistics of fluorescence lifetimes and their corresponding amplitudes obtained from 6 measurements on the palm for a single subject at an emission wavelength of 442 nm.

Parameter	**Mean Value**	**Standard Deviation**	**Coefficient of Variation**
Fluorescence Lifetime τ_1 (ns)	0.409	0.029	7.09%
Amplitude A_1	0.783	0.013	1.66 %
Fluorescence Lifetime τ_2 (ns)	2.591	0.129	4.98%
Amplitude A_2	0.183	0.008	4.37%
Fluorescence Lifetime τ_3	8.880	0.410	4.62 %
Amplitude A_3	0.034	0.005	14.71%

Table 3. Statistics of fluorescence lifetimes and their corresponding amplitudes obtained on the left palm of 35 subjects at an emission wavelength of 442 nm.

Parameter	Mean Value	Standard Deviation
Fluorescence Lifetime τ_1 (ns)	0.435	0.091
Amplitude A_1	0.786	0.042
Fluorescence Lifetime τ_2 (ns)	2.674	0.291
Amplitude A_2	0.181	0.035
Fluorescence Lifetime τ_3	9.415	1.533
Amplitude A_3	0.033	0.010